

# Reinforcement Learning for Microcanonical Graph Ensemble with Assortativity Constraints

Hoyun Choi<sup>1</sup>, Junghyo Jo<sup>1,2,3</sup>, Deok-Sun Lee<sup>1,4\*</sup>

<sup>1</sup>School of Computational Sciences, Korea Institute for Advanced Study, 85, Hoegi-ro, 02455, Seoul, Korea.

<sup>2</sup>Department of Physics Education, Seoul National University, 1, Gwanak-ro, 08826, Seoul, Korea.

<sup>3</sup>Center for Theoretical Physics and Artificial Intelligence Institute, Seoul National University, 1, Gwanak-ro, 08826, Seoul, Korea.

<sup>4</sup>Center for AI and Natural Sciences, Korea Institute for Advanced Study, 85, Hoegi-ro, 02455, Seoul, Korea.

\*Corresponding author(s). E-mail(s): [deoksunlee@kias.re.kr](mailto:deoksunlee@kias.re.kr);  
Contributing authors: [hychoi@kias.re.kr](mailto:hychoi@kias.re.kr); [jojunghyo@snu.ac.kr](mailto:jojunghyo@snu.ac.kr);

## Abstract

How network structure determines function is a fundamental question, and it can be investigated by graph ensembles with precisely controlled structural properties. Canonical approaches, formulated as exponential random graph models (ERGMs), enforce constraints only in expectation, allowing individual realizations to fluctuate around the target. Conversely, microcanonical ensembles impose hard constraints exactly, but practical sampling methods beyond fixing the degree sequence have remained out of reach. Here we introduce the Deep Microcanonical Graph Generator (DMGG), a reinforcement learning (RL) framework that transforms any given graph through degree-preserving rewirings to exactly reach a prescribed assortativity, which characterizes the degree–degree correlation of adjacent nodes. Instead of relying on the entropically dominated Metropolis–Hastings dynamics of the ERGM, DMGG employs a policy-guided search that maximally alters the joint-degree matrix. This eliminates exhaustive parameter tuning and accelerates generation by at least an order of magnitude while preserving configurational diversity. As DMGG generalizes across various graph sizes, sparsities, and topologies, it provides exact null models that allow for the quantitative isolation of secondary observables, such as the clustering coefficient. These results establish RL as a practical and powerful paradigm for generating hard-constrained graphs, opening avenues to investigate structure–function relationships free from ensemble artifacts.

The ensemble of random graphs under selected constraints provides a natural null model to assess the significance of observed features of real-world networks and to investigate how the imposed constraints influence structural and dynamical properties. As in statistical mechanics, distinct

ensembles can be employed depending on how constraints are imposed. Canonical ensembles, formulated as exponential random graph models (ERGMs), enforce constraints only in expectation

(*soft constraints*) [1–3]. In contrast, microcanonical ensembles enforce them exactly in every realization (*hard constraints*) [4]. A familiar example is the degree sequence, which is constrained only on average in ERGM but fixed exactly in the configuration model [5, 6].

In finite systems, canonical ensembles introduce structural fluctuations over different realizations that can obscure the effects of the imposed constraints. In the thermodynamic limit, inequivalence between canonical and microcanonical graph ensembles arises even in simple graphs with fixed degree sequences [7, 8]. Under multiply constrained systems like the edge–triangle model [9, 10], canonical formulations can exhibit discontinuous phase transitions that bypass intermediate graph configurations, which remain accessible in the corresponding microcanonical ensemble. Therefore, residual fluctuations and configurational inaccessibility under soft constraints establish a critical need for generative methods that can efficiently generate graphs under hard constraints.

While a given degree sequence can be preserved by degree-preserving rewiring, as in the configuration model, generating graphs that exactly preserve properties beyond the degree sequence is difficult to implement, hindering the construction of microcanonical ensembles. In this study, we focus on assortativity  $\rho$ , the degree–degree correlation of adjacent nodes [11]. Assortativity is a fundamental structural property, affecting percolation criticality [12, 13], synchronization and spreading dynamics [14–16], and robustness [17]. Yet, generating graph ensembles that strictly satisfy an arbitrary target assortativity  $\rho^*$  poses a formidable challenge. Although a sampling method that preserve a given joint-degree matrix have been proposed [18], determining how to generate an ensemble of joint-degree matrices that matches a given  $\rho^*$  remains open. Meanwhile, heuristic rewirings [19], like canonical ERGMs, rely on soft constraints leaving residual fluctuations and require nontrivial parameter tuning.

Given these difficulties, modern deep learning offers alternative data-driven graph generators based on autoregressive [20, 21], VAE [22, 23], GAN [24, 25], and diffusion [26, 27]. These

approaches can be steered toward desired properties via conditional generation [24, 28] or optimized for specific goals using reinforcement learning (RL), such as RNet–DQN [29] and ResiNet [30] for robust network design. For microcanonical graph ensemble generation, however, two obstacles dominate: representative training data that strictly satisfy constraints are scarce, and approximate conditional control is insufficient when exact compliance is required.

Here we introduce the *Deep Microcanonical Graph Generator* (DMGG), a practical deep RL framework for hard constraint graph generation, with assortativity as a showcase. It navigates the configuration space of graphs via degree-preserving rewiring, to achieve assortativity  $\rho$  sufficiently close to a target  $\rho^*$ , i.e.,  $|\rho - \rho^*| < \varepsilon$  at a prescribed precision  $\varepsilon$ . Unlike supervised generative models, DMGG requires no training dataset of pre-existing graphs spanning various values of  $\rho$ . Instead, it learns the optimal rewiring policy  $\pi$  solely from reward signals based on the gap between current and target assortativities. Consequently, it reduces the required rewirings by at least an order of magnitude compared to ERGM while retaining substantial configurational diversity. Moreover, once trained, DMGG reliably delivers prescribed precision across diverse assortativities, sizes, sparsities and topologies of initial graphs. We investigate how the joint-degree matrix evolves in ERGM and DMGG to elucidate how the latter achieves such accelerated graph generation.

## From canonical to microcanonical ensemble

For a simple graph  $G = (\mathcal{V}, \mathcal{E})$  with  $N = |\mathcal{V}|$  nodes and  $E = |\mathcal{E}|$  edges, assortativity is defined as the Pearson correlation coefficient between the degrees at the endpoints of each edge,

$$\rho = \frac{\frac{1}{E} \sum_{(i,j) \in \mathcal{E}} k_i k_j - \mu^2}{\frac{1}{2E} \sum_{(i,j) \in \mathcal{E}} (k_i^2 + k_j^2) - \mu^2}, \quad (1)$$

where  $k_i$  is the degree of node  $i$  and  $\mu \equiv \sum_{(i,j) \in \mathcal{E}} (k_i + k_j) / 2E$  [31, 32].

To generate canonical and microcanonical ensembles constrained on  $\rho$  within the configuration space of a fixed degree sequence, we employ

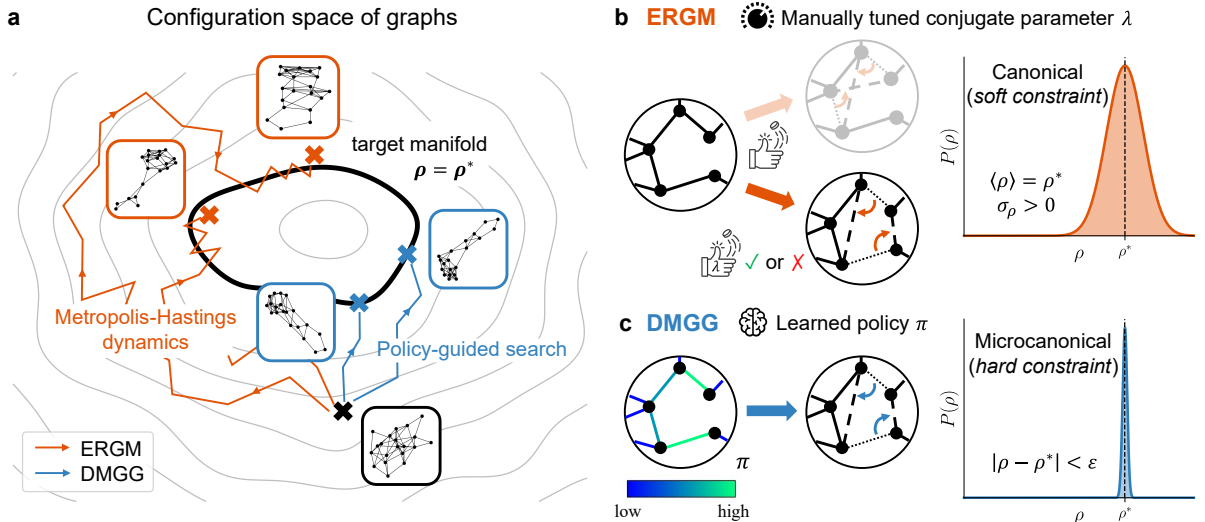


**Fig. 1 Comparison between canonical (ERGM) and microcanonical (DMGG) graph generation under assortativity  $\rho$  constraints.** **a**, Schematic representation of ERGM and DMGG navigating the configuration space of graphs for a given degree sequence, where each contour line indicates a set of graphs sharing the same  $\rho$ . Starting from an initial graph, both ERGM and DMGG traverse the space through sequences of rewirings. ERGM approaches the target manifold  $\{G|\rho(G) = \rho^*\}$  via stochastic Metropolis–Hastings dynamics, whereas DMGG uses policy-guided search that reaches the constraint more efficiently. **b**, In ERGM, randomly sampled rewiring proposals are accepted or rejected according to the manually tuned conjugate parameter  $\lambda$ . The resulting graphs form a canonical ensemble satisfying the soft constraint  $\langle \rho \rangle = \rho^*$ , in which  $\rho$  fluctuates around  $\rho^*$  and yields a distribution  $P(\rho)$  with finite variance  $\sigma_\rho > 0$ . **c**, In DMGG, a learned policy  $\pi$  assigns scores to edges to select the rewiring that effectively navigates the graph toward  $\rho^*$ . Generated graphs satisfy the hard constraint  $|\rho - \rho^*| < \varepsilon$ , yielding a sharply localized  $P(\rho)$ .

degree-preserving rewiring for both ERGM and DMGG. Before applying either models, we first randomize the input graph via the configuration model to eliminate any structural biases inherited from the initial topology. During the rewiring process, two distinct edges are chosen and their endpoints are reconnected in one of the two possible pairings, discarding moves that create self-loops, multiedges, or leave the topology unchanged. By strictly maintaining the degree sequence, this rewire isolates the effects of degree–degree correlations from underlying degree heterogeneity.

The ERGM employs these rewirings within a Metropolis–Hastings (MH) chain [33, 34] driven by a conjugate parameter  $\lambda$ . As illustrated in Fig. 1a and b, randomly proposed rewiring from the current graph  $G$  to a new graph  $G'$  is accepted with probability

$$\min[1, \exp(\lambda \Delta K)], \quad (2)$$

where  $K(G) \equiv \sum_{(i,j) \in \mathcal{E}} k_i k_j$  and  $\Delta K \equiv K(G') - K(G)$ . Note that for a fixed degree sequence,  $\rho(G)$

is linearly related to  $K(G)$ . Thus, utilizing the unnormalized sum  $K$  provides a direct and computationally simpler proxy for  $\rho$ . This accept–reject process is repeated until the  $\rho$  reaches equilibrium (see Methods). Note that the ERGM ensemble generated from a single initial graph is microcanonical in the degree sequence but canonical in assortativity. While theoretically well grounded, the canonical baseline is hindered by the lack of a universal mapping between  $\rho$  and  $\lambda$ . Consequently, applying this method requires costly parameter tuning for each degree sequence and target, and often requires an excessive number of rewirings to reach the desired state.

DMGG reformulates graph generation as a Markov decision process [35, 36], replacing the stochastic proposal and acceptance–rejection steps of MH dynamics with a policy-guided search. Starting from the randomized initial graph, a learned policy  $\pi$ , obtained by the training procedure described below, sequentially selects rewiring actions that efficiently navigate the graph toward

Property	Training	Evaluation
Size ( $N$ )	$[10^2, 10^3]$	$[10^2, 10^4]$
Sparsity ( $\langle k \rangle$ )	$[3, 10]$	$[3, 20]$
Topology	WS, ER, BA	WS, ER, SBM, RGG, CL, HK, BA
Assortativity ( $\rho$ )	$[-0.5, 0.5]$	$[-0.8, 0.8]$
Tolerance ( $\varepsilon$ )	0.005	0.001

**Table 1 Training and evaluation domains for DMGG.** To reduce computational cost, training is restricted to small, sparse networks from three random graph models: Watts–Strogatz (WS), Erdős–Rényi (ER), and Barabási–Albert (BA). The target assortativity  $\rho$  is sampled from a narrow range with a loose tolerance  $\varepsilon$ . The evaluation domain is significantly broader, encompassing larger and denser systems, a wider target range, stricter tolerances, and unseen topologies with distinct structural features, such as the stochastic block model (SBM), random geometric graph (RGG), Chung–Lu (CL), and Holme–Kim (HK) models.

the target (Fig. 1a and c). These targeted modifications continue until the graph satisfies the hard constraint  $|\rho - \rho^*| < \varepsilon$ .

To minimize the training cost, it is restricted to small, sparse graphs from three foundational random graph models (Watts–Strogatz (WS) [37], Erdős–Rényi (ER) [38], and Barabási–Albert (BA) [39]), alongside a narrow target range and a loose tolerance (Tab. 1). Training is performed using Proximal Policy Optimization (PPO) [40], completed after approximately  $5 \times 10^7$  rewirings, or  $3 \times 10^5$  graph generations, requiring less than 24 hours on a single NVIDIA A100 GPU. Once trained, the model is evaluated on a significantly broader domain that encompasses larger and denser systems, diverse unseen topologies, a wider assortativity range, and stricter tolerances. Details regarding the RL formulation, including neural network architectures, rewards, and training procedures, are provided in Methods.

We first compare the DMGG against ERGM when the initial graph is an ER graph with  $N = 1000$  and  $E = 3000$ . Both methods eventually approach the prescribed assortativities in the range of  $[-0.8, 0.8]$ , but their paths differ qualitatively. Fig. 2a and b compare representative trajectories of  $\rho$  as a function of the number of rewirings  $t$  during the generation process. Because

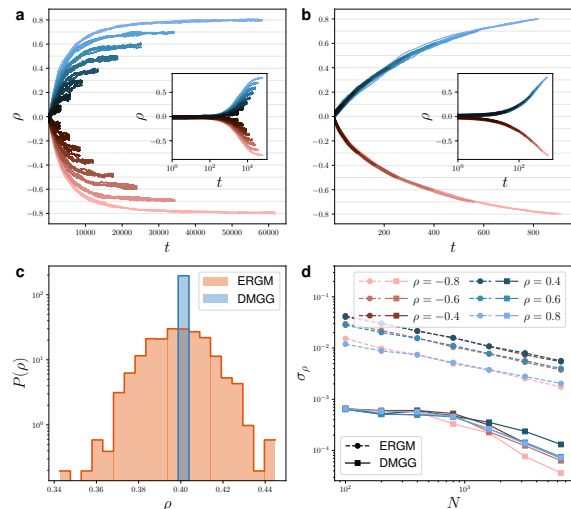


**Fig. 2 Convergence and precision in assortativity-constrained graph generation.** a, b, Evolution of assortativity  $\rho$  during the generation process of ERGM and DMGG, respectively. Starting from an initial Erdős–Rényi (ER) graph ( $N = 1000$  and  $E = 3000$ ) with neutral assortativity ( $\rho \approx 0$ ), five trajectories for each target (indicated by color) are shown. Insets illustrate the same trajectories on a logarithmic time scale. c, Distribution of  $\rho$  measured over 1000 generated graphs with target assortativity  $\rho^* = 0.4$ . d, Standard deviation of assortativity  $\sigma_\rho$  versus system size  $N$ , with the same color scheme as in a and b. Dashed lines with circle markers and solid lines with square markers correspond to ERGM and DMGG, respectively. Results are shown for ER graphs in which the mean degree is fixed at 6 across all system sizes.

the ERGM follows MH dynamics governed by a conjugate parameter  $\lambda$  specific to each target, it exhibits distinct trajectories. In contrast, DMGG uses a single policy  $\pi$  whose dominant control signal is the direction toward the target, causing trajectories with the same sign of target to collapse onto a universal path. This offers a significant practical advantage, as a single generation process can simultaneously generate graphs with a range of  $\rho$ .

Fig. 2c compares the distribution  $P(\rho)$  of the generated graphs for the  $\rho^* = 0.4$  case. The ERGM satisfies only soft constraints, producing a broad distribution centered near the target. In contrast, the distribution from DMGG is sharply concentrated around the target value with tolerance  $\varepsilon = 0.001$ . As shown in Fig. 2d, the standard deviation  $\sigma_\rho$  of the canonical ensemble decreases with system size  $N$  at a fixed mean degree  $\langle k \rangle = 6$  [41]. For DMGG,  $\sigma_\rho$  is inherently

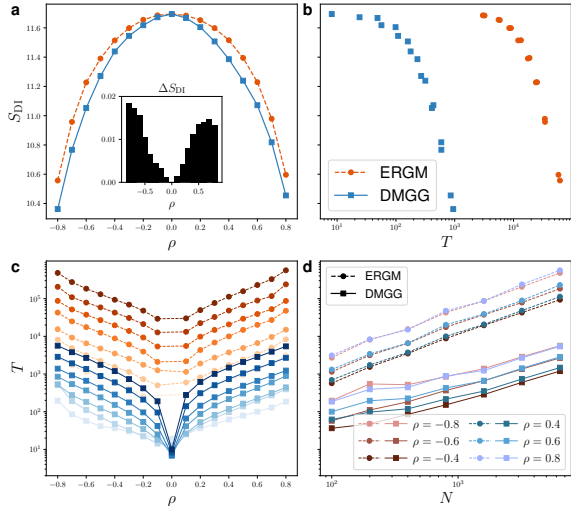


**Fig. 3 Configurational diversity and computational efficiency of DMGG.** **a**, Dyad-independent entropy  $S_{\text{DI}}(\{p_{ij}\})$  measured in the ensembles generated by ERGM and DMGG, as a function of assortativity  $\rho$ . The inset shows the deviation for each  $\rho$ ,  $\Delta S_{\text{DI}} \equiv (S_{\text{DI}}^{\text{ERGM}} - S_{\text{DI}}^{\text{DMGG}}) / S_{\text{DI}}^{\text{ERGM}}$ . **b**, Parametric plot of  $S_{\text{DI}}$  as a function of the number of required rewirings  $T$ , where each marker corresponds to the data for a distinct assortativity in **a**. **c**,  $T$  as a function of target assortativity  $\rho$  with system sizes  $N = 100, 200, \dots, 6400$  indicated by color gradient (light to dark). **d**, Scaling of  $T$  with system size  $N$  for fixed targets (colors). Dashed lines with circle markers and solid lines with square markers correspond to ERGM and DMGG, respectively. All results are shown for ER graphs with a fixed mean degree  $\langle k \rangle = 6$ .

bounded by the tolerance  $\varepsilon$  and decreases further as  $N$  increases, remaining smaller than that of ERGM. This is because  $\pi$  is trained to minimize the gap  $|\rho - \rho^*|$  even within the tolerance window, and larger systems allow for finer control as each rewiring modifies  $\rho$  by only  $O(E^{-1})$ .

## Ensemble diversity with accelerated generation

An ensemble generator would be of limited scientific value if it collapsed onto only a few specific realizations rather than exploring a substantial portion of the accessible configuration space. We therefore examine whether DMGG retains sufficient configurational diversity while remaining practically efficient.

Since exhaustive graph construction and direct estimation of Shannon entropy is intractable for large graph configuration spaces, we quantify

ensemble diversity using the dyad-independent entropy:

$$S_{\text{DI}} \equiv -\frac{2}{E} \sum_{i < j} [p_{ij} \ln p_{ij} + (1 - p_{ij}) \ln(1 - p_{ij})], \quad (3)$$

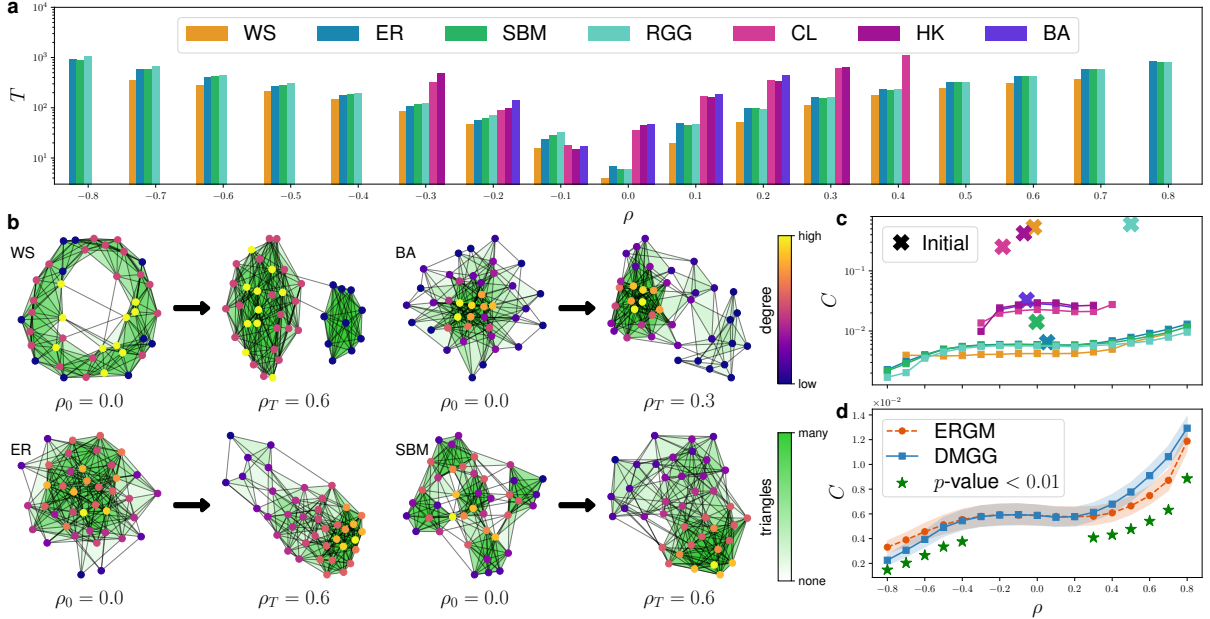
where  $p_{ij}$  denotes the marginal probability that an edge exists between nodes  $i$  and  $j$ . By assuming statistical independence between edges,  $S_{\text{DI}}$  provides an upper bound on the Shannon entropy of degree constrained ensembles, as the fixed degree sequence can impose correlations. This proxy quantifies whether the generated graphs collapse onto a narrow subset of configurations, while not necessarily guaranteeing unbiased sampling of the constrained graph space. Fig. 3a shows the  $S_{\text{DI}}$  from ERGM and DMGG ensembles starting from a single initial ER graph ( $N = 1000$  and  $E = 3000$ ). For each target assortativity, we generate 1000 graph instances from separate runs and measure  $p_{ij}$ . The estimated  $S_{\text{DI}}$  decreases as  $|\rho|$  increases, consistent with the expectation that the accessible graph space shrinks under stronger constraints. As DMGG enforces a hard constraint, its entropy is inherently smaller than that of the ERGM. Crucially, however, the DMGG and ERGM curves nearly overlap, with a deviation  $\Delta S_{\text{DI}} \equiv (S_{\text{DI}}^{\text{ERGM}} - S_{\text{DI}}^{\text{DMGG}}) / S_{\text{DI}}^{\text{ERGM}}$  remaining below 2% across the entire assortativity range (inset).

Fig. 3b demonstrates that DMGG reaches this high-diversity regime with significantly fewer computational cost than the ERGM, quantified by the required number of rewirings  $T$  (see Methods). Thus, in DMGG, hard constraint satisfaction, configurational diversity, and efficient generation are achieved simultaneously.

We systematically quantify this computational efficiency using ER graphs with a fixed mean degree  $\langle k \rangle = 6$ . As shown in Figs. 3c and d, DMGG consistently requires at least an order of magnitude fewer rewirings  $T$  than the ERGM across all target  $\rho \in [-0.8, 0.8]$  and system sizes  $N = 100, 200, \dots, 6400$ . We fit the generation cost  $T(\rho, N)$  as

$$T \sim 10^{\alpha|\rho|} N^{\beta}, \quad (4)$$

with exponents  $\alpha_{\text{ERGM}} = 1.51 \pm 0.08$  and  $\beta_{\text{ERGM}} = 1.14 \pm 0.29$  for the ERGM, compared with  $\alpha_{\text{DMGG}} = 1.56 \pm 0.26$  and  $\beta_{\text{DMGG}} = 0.86 \pm 0.22$  for DMGG. The exponential dependence



**Fig. 4 Generalization of DMGG across diverse graph families.** **a**, Number of rewirings  $T$  required to reach target assortativity  $\rho$  in different initial topologies. Missing bars indicate target  $\rho$  values outside the physically feasible range of a given topology. **b**, Representative examples of graph transformation by DMGG. The initial graphs (left) with diverse topologies with assortativity  $\rho_0 \approx 0$  are rewired into target configurations (right) with prescribed assortativities  $\rho_T$ . Node colors indicate relative degrees, and triangles contributing to the clustering coefficient  $C$  are shaded green. **c**, Average  $C$  of the generated ensembles from DMGG as a function of  $\rho$ , using the same color scheme as in **a** to denote topology.  $(\rho, C)$  of the initial graphs are marked by crosses. **d**,  $C(\rho)$  for ERGM and DMGG ensembles generated from the same initial ER graph ( $N = 1000$  and  $E = 3000$ ). Shaded areas indicate the interquartile range, and green stars mark  $\rho$  where the difference in  $C$  between two ensembles is statistically significant ( $p < 0.01$ ).

on  $|\rho|$  reflects the extensive structural reorganization required to reach extreme assortativities. Meanwhile, the near-linear scaling with  $N$  is theoretically expected, as a single rewiring adjusts  $\rho$  by  $O(E^{-1})$ . Crucially, these scaling behaviors suggest that the speedup of DMGG persists asymptotically, extending to larger graphs beyond those examined in our experiments.

## Generalization across topologies

Here we generate microcanonical ensembles using the DMGG, with various families of initial graphs covering the full spectrum of degree heterogeneity. Specifically, we consider (1) *narrow distributions* represented by WS small-world graphs; (2) *Poisson-like distributions*, including ER random graphs, stochastic block models (SBM) [42] with community structure, and spatially clustered random geometric graphs (RGG) [43]; and (3)

*heavy-tailed distributions*, encompassing scale-free BA graphs, Chung–Lu (CL) models [44] with controllable degree exponent, Holme–Kim (HK) models [45] with high clustering. Throughout, target assortativities are chosen within the empirically feasible range of each degree sequence. Unlike ERGMs, which require exhaustive, case-by-case parameter tuning for each initial topology and system size, a single pre-trained DMGG model can be applied across all these diverse structures without any retraining.

As initial graphs are randomized via the configuration model and their assortativity starts near zero, the number of rewiring steps  $T$  required to reach a target assortativity naturally increases with  $|\rho|$  (Fig. 4a). Notably, the  $T(\rho)$  profiles are primarily governed by the degree distribution. While WS model with the narrowest degree distribution requires the fewest rewirings, models with Poisson-like distributions (ER, SBM, and RGG) exhibit slightly higher  $T$ . Graphs characterized by

broad, heavy-tailed degree distributions (CL, HK, and BA) demand significantly more rewirings.

To visually demonstrate structural evolution, Fig. 4b shows representative transformations of small graphs ( $N = 40$  and  $E = 200$ ). As DMGG drives the networks toward high assortativity, high degree nodes converge into tightly interconnected central cores. Furthermore, networks sharing similar degree distributions, such as ER and SBM, evolve into comparable structures.

By completely eliminating the computational bottleneck of parameter tuning, this generalizability establishes DMGG as a highly versatile framework for generating hard constrained null models. Consequently, it enables systematic investigations into how primary constraints, such as the degree sequence and  $\rho$ , influence secondary structural observables. As a demonstration, Fig. 4c compares the average clustering coefficient  $C$  of various initial graphs and their corresponding DMGG-generated ensembles as a function of  $\rho$ . Within the generated ensembles, the  $C(\rho)$  curves group distinctly according to the degree distribution. In configuration models without degree-degree correlation, clustering is calculated approximately as  $C \approx (\langle k^2 \rangle - \langle k \rangle)^2 / N \langle k \rangle^3$ . Accordingly, networks with heavy-tailed distributions (CL, HK, BA) inherently exhibit larger clustering due to their diverging second moments. While this is well established for neutral assortativity ( $\rho = 0$ ), our results demonstrate that this disparities persist across varying  $\rho$ . Furthermore, while the ensembles provide the baseline  $C$  depending solely by the degree sequence and assortativity, the initial graphs often display higher  $C$  driven by their specific generative mechanisms, such as spatial embeddings (RGG) or explicit triad formation (HK). By providing microcanonical ensemble, DMGG thus allows to rigorous quantification of structural features that cannot be explained by these primary constraints alone.

On the other hand, Fig. 4d highlights the impact of constraint stringency by comparing ERGM and DMGG ensembles initialized from a single ER graph. While both ensembles share similar  $C(\rho)$  trends, we observe that the variation of  $C$  is more pronounced under DMGG. The differences between the two ensembles are statistically significant across the large  $|\rho|$  regime ( $p < 0.01$ ), indicating that discrepancies between

canonical and microcanonical ensembles become robust when strong constraints are enforced.

## Directed flux in the configuration space

To trace the origin of DMGG’s speedup, we investigate the joint-degree matrix  $J$ , where  $J_{k_1 k_2}$  denotes the number of edges connecting nodes of degrees  $k_1$  and  $k_2$  [18]. We define the flux  $\Delta J$  as the expected change in  $J$  per rewiring step:  $\Delta J_{k_1 k_2}(t) \equiv \langle J_{k_1 k_2}(t+1) - J_{k_1 k_2}(t) \rangle$ . Snapshots of  $J$  and  $\Delta J$  during the ERGM and DMGG generation processes for a target  $\rho^* = 0.8$  are shown in Fig. 5.

As illustrated in Figs. 5a and b, both ERGM and DMGG traverse similar sequences of  $J$  matrices, confirming that they reach comparable macroscopic structures. However, the fluxes  $\Delta J$  shown in Figs. 5c and d reveal fundamentally distinct strategies. Qualitatively, ERGM proposals are drawn uniformly from all admissible rewires. This inherently concentrates  $\Delta J$  around the bright region in Fig. 5c, where the joint-degree distribution is peaked, representing the entropic bias. In contrast, DMGG bypasses this by explicitly targeting high-impact, off-diagonal degree pairs that maximally alter  $\rho$ . Quantitatively, the ERGM flux is attenuated by stochastic fluctuations and MH rejections, whereas the learned policy in DMGG induces more directed flux, approximately 40 times larger in magnitude of  $\Delta J$ , thereby reaching the target assortativity in an order of magnitude fewer rewirings.

This mechanism clarifies that the acceleration arises from a fundamental shift in the navigation dynamics within the configuration space. The ERGM approaches the target via an entropically dominated random walk, spending significant time exploring abundant but low-impact local moves. In contrast, DMGG executes a directed transport, effectively identifying the sparse subset of rewirings that constitute the most efficient route to the target manifold. Consequently, the model achieves efficiency by replacing a slow diffusive relaxation with a guided search driven by the learned policy.

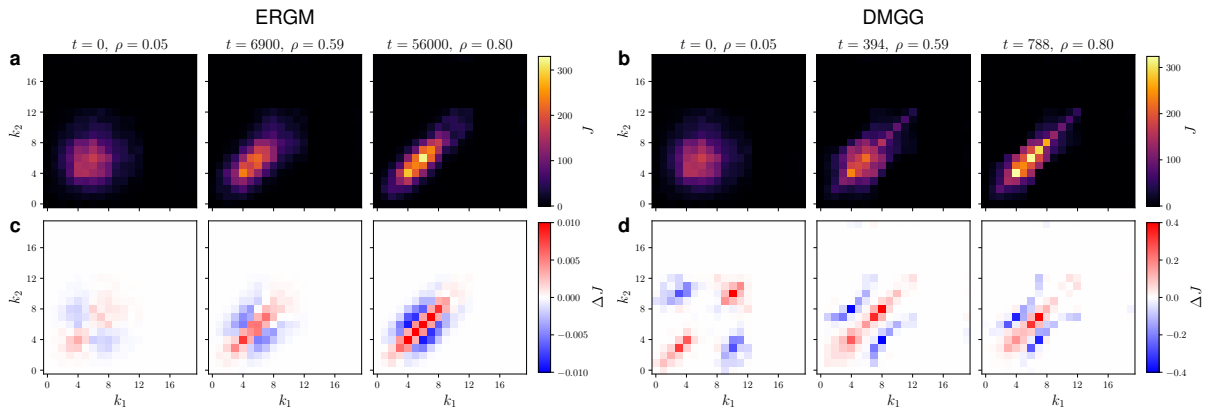


**Fig. 5** Rewiring strategies of ERGM and DMGG. Snapshots of the joint-degree matrix  $J$  (top row) and its expected change per rewiring  $\Delta J$  (bottom row) during the generation process with target  $\rho^* = 0.8$ . **a, c**, ERGM dynamics driven by the Metropolis–Hastings process. **b, d**, DMGG dynamics driven by a policy-guided process.

## Beyond degree correlations

The main contribution of this work is methodological: a deep RL framework that can generate graph instances that satisfy a user-specified hard assortativity constraint across a wide range of graph sizes and topologies without relying on pre-computed constrained training data. Under the diagnostics used here, the resulting ensembles retain substantial configurational diversity, and Fig. 4c provides a proof of principle that soft and hard constrained ensembles can exhibit visibly different trends in a secondary observable such as clustering coefficients.

Although we focus on assortativity constraint with degree-preserving rewiring, the same framework could in principle be adapted to other graph properties, provided that the target observable can be evaluated efficiently and that a valid action set is available to modify it. This includes local observables such as the average clustering coefficient and motif counts, or global metrics such as diameter and algebraic connectivity. Extensions to multiple constraints would offer a route to probe regimes where ERGM struggles with phase coexistence and ensemble non-equivalence. Furthermore, applications to enriched graph classes, such as bipartite, spatially embedded, multilayer graphs, and hypergraphs, remain promising but would require corresponding constraint evaluations and action designs.

## References

- [1] Jaynes, E.T.: Information theory and statistical mechanics. *Phys. Rev.* **106**(4), 620 (1957)
- [2] Frank, O., Strauss, D.: Markov graphs. *J. Am. Stat. Assoc.* **81**(395), 832–842 (1986)
- [3] Park, J., Newman, M.E.: Statistical mechanics of networks. *Phys. Rev. E* **70**(6), 066117 (2004)
- [4] Bianconi, G.: Entropy of network ensembles. *Phys. Rev. E* **79**(3), 036114 (2009)
- [5] Fosdick, B.K., Larremore, D.B., Nishimura, J., Ugander, J.: Configuring random graph models with fixed degree sequences. *SIAM Rev.* **60**(2), 315–355 (2018)
- [6] Newman, M.E., Strogatz, S.H., Watts, D.J.: Random graphs with arbitrary degree distributions and their applications. *Phys. Rev. E* **64**(2), 026118 (2001)
- [7] Squartini, T., Mol, J., Hollander, F., Garlaschelli, D.: Breaking of ensemble equivalence in networks. *Phys. Rev. Lett.* **115**(26), 268701 (2015)
- [8] Squartini, T., Mastrandrea, R., Garlaschelli, D.: Unbiased sampling of network ensembles. *New J. Phys.* **17**(2), 023052 (2015)

- [9] Radin, C., Yin, M.: Phase transitions in exponential random graphs. *Ann. Appl. Probab.*, 2458–2471 (2013)
- [10] Chatterjee, S., Diaconis, P.: Estimating and understanding exponential random graph models. *Ann. Stat.* **41**(5), 2428–2461 (2013)
- [11] Newman, M.E.: The structure and function of complex networks. *SIAM Rev.* **45**(2), 167–256 (2003)
- [12] Noh, J.D.: Percolation transition in networks with degree-degree correlation. *Phys. Rev. E* **76**(2), 026116 (2007)
- [13] Goltsev, A.V., Dorogovtsev, S.N., Mendes, J.F.: Percolation on correlated networks. *Phys. Rev. E* **78**(5), 051105 (2008)
- [14] Van Mieghem, P., Wang, H., Ge, X., Tang, S., Kuipers, F.A.: Influence of assortativity and degree-preserving rewiring on the spectra of networks. *Eur. Phys. J. B* **76**(4), 643–652 (2010)
- [15] Avalos-Gaytán, V., Almendral, J.A., Papo, D., Schaeffer, S.E., Boccaletti, S.: Assortative and modular networks are shaped by adaptive synchronization processes. *Phys. Rev. E* **86**(1), 015101 (2012)
- [16] Boguná, M., Pastor-Satorras, R.: Epidemic spreading in correlated complex networks. *Phys. Rev. E* **66**(4), 047104 (2002)
- [17] Zhou, D., Stanley, H.E., D’Agostino, G., Scala, A.: Assortativity decreases the robustness of interdependent networks. *Phys. Rev. E* **86**(6), 066103 (2012)
- [18] Bassler, K.E., Del Genio, C.I., Erdős, P.L., Miklós, I., Toroczkai, Z.: Exact sampling of graphs with prescribed degree correlations. *New J. Phys.* **17**, 083052 (2015)
- [19] Xulvi-Brunet, R., Sokolov, I.M.: Reshuffling scale-free networks: From random to assortative. *Phys. Rev. E* **70**(6), 066102 (2004)
- [20] You, J., Ying, R., Ren, X., Hamilton, W., Leskovec, J.: GraphRNN: Generating realistic graphs with deep auto-regressive models. In: *Proceedings of the 35th International Conference on Machine Learning (ICML)*, vol. 80 (2018)
- [21] Liao, R., Li, Y., Song, Y., Wang, S., Hamilton, W.L., Duvenaud, D., Urtasun, R., Zemel, R.: Efficient graph generation with graph recurrent attention networks. In: *Proceedings of the 33rd Conference on Neural Information Processing Systems (NeurIPS)*, vol. 32 (2019)
- [22] Simonovsky, M., Komodakis, N.: Graphvae: Towards generation of small graphs using variational autoencoders. In: *Proceedings of the 27th International Conference on Artificial Neural Networks (ICANN)*, Rhodes, Greece (2018)
- [23] Jin, W., Barzilay, R., Jaakkola, T.: Junction tree variational autoencoder for molecular graph generation. In: *Proceedings of the 35th International Conference on Machine Learning (ICML)*, vol. 80 (2018)
- [24] De Cao, N., Kipf, T.: MolGAN: An implicit generative model for small molecular graphs. In: *Workshop on Theoretical Foundations and Applications of Deep Generative Models at the 35th International Conference on Machine Learning (ICML)* (2018)
- [25] Martinkus, K., Loukas, A., Perraudin, N., Wattenhofer, R.: SPECTRE: Spectral conditioning helps to overcome the expressivity limits of one-shot graph generators. In: *Proceedings of the 39th International Conference on Machine Learning (ICML)*, vol. 162 (2022)
- [26] Vignac, C., Krawczuk, I., Siraudin, A., Wang, B., Cevher, V., Frossard, P.: DiGress: Discrete denoising diffusion for graph generation. In: *Proceedings of the Eleventh International Conference on Learning Representations (ICLR)* (2023)
- [27] Huang, H., Sun, L., Du, B., Fu, Y., Lv, W.: GraphGDP: Generative diffusion processes for permutation invariant graph generation.

- In: Proceedings of the 22nd IEEE International Conference on Data Mining (ICDM) (2022)
- [28] Gómez-Bombarelli, R., Wei, J.N., Duvenaud, D., Hernández-Lobato, J.M., Sánchez-Lengeling, B., Sheberla, D., Aguilera-Iparraguirre, J., Hirzel, T.D., Adams, R.P., Aspuru-Guzik, A.: Automatic chemical design using a data-driven continuous representation of molecules. *ACS Cent. Sci.* **4**(2), 268–276 (2018)
- [29] Darvari, V.-A., Hailes, S., Musolesi, M.: Goal-directed graph construction using reinforcement learning. *Proceedings of the Royal Society A: Mathematical, Physical and Engineering Sciences* **477**(2254) (2021)
- [30] Yang, S., KAILI, M., Wang, B., Yu, T., Zha, H.: Learning to boost resilience of complex networks via neural edge rewiring. *Transactions on Machine Learning Research* (2023)
- [31] Newman, M.E.: Assortative mixing in networks. *Phys. Rev. Lett.* **89**(20), 208701 (2002)
- [32] Newman, M.E.: Mixing patterns in networks. *Phys. Rev. E* **67**(2), 026126 (2003)
- [33] Metropolis, N., Rosenbluth, A.W., Rosenbluth, M.N., Teller, A.H., Teller, E.: Equation of state calculations by fast computing machines. *J. Chem. Phys.* **21**(6), 1087–1092 (1953)
- [34] Hastings, W.K.: Monte carlo sampling methods using markov chains and their applications. *Biometrika* **57**(1), 97–109 (1970)
- [35] Bellman, R.: A markovian decision process. *J. Math. Mech.*, 679–684 (1957)
- [36] Sutton, R.S., Barto, A.G.: Reinforcement learning: An introduction. *IEEE Trans. Neural Netw.* **9**(5), 1054–1054 (1998)
- [37] Watts, D.J., Strogatz, S.H.: Collective dynamics of 'small-world' networks. *Nature* **393**(6684), 440–442 (1998)
- [38] Erdős, P., Rényi, A.: On the evolution of random graphs. *Publ. Math. Inst. Hungar. Acad. Sci* **5**(1), 17–61 (1960)
- [39] Barabási, A.-L., Albert, R.: Emergence of scaling in random networks. *Science* **286**(5439), 509–512 (1999)
- [40] Schulman, J., Wolski, F., Dhariwal, P., Radford, A., Klimov, O.: Proximal policy optimization algorithms. *arXiv preprint arXiv:1707.06347* (2017)
- [41] Touchette, H.: Equivalence and nonequivalence of ensembles: Thermodynamic, macrostate, and measure levels. *J. Stat. Phys.* **159**, 987–1016 (2015)
- [42] Holland, P.W., Laskey, K.B., Leinhardt, S.: Stochastic blockmodels: First steps. *Social Networks* **5**(2), 109–137 (1983)
- [43] Dall, J., Christensen, M.: Random geometric graphs. *Phys. Rev. E* **66**(1), 016121 (2002)
- [44] Chung, F., Lu, L.: The average distances in random graphs with given expected degrees. *Proc. Natl. Acad. Sci. USA* **99**(25), 15879–15882 (2002)
- [45] Holme, P., Kim, B.J.: Growing scale-free networks with tunable clustering. *Phys. Rev. E* **65**(2), 026107 (2002)
- [46] Tavakoli, A., Pardo, F., Kormushev, P.: Action branching architectures for deep reinforcement learning. In: *Proceedings of the 32nd AAAI Conference on Artificial Intelligence (AAAI)*, vol. 32 (2018)
- [47] Huang, S., Ontañón, S.: A closer look at invalid action masking in policy gradient algorithms. In: *Proceedings of the 35th International Florida Artificial Intelligence Research Society Conference (FLAIRS)* (2022)
- [48] Xu, K., Hu, W., Leskovec, J., Jegelka, S.: How powerful are graph neural networks? In: *Proceedings of the 7th International Conference on Learning Representations (ICLR)* (2019)

- [49] Perez, E., Strub, F., De Vries, H., Dumoulin, V., Courville, A.: FiLM: Visual reasoning with a general conditioning layer. In: Proceedings of the 32nd AAAI Conference on Artificial Intelligence (AAAI), vol. 32 (2018)
- [50] Pathak, D., Agrawal, P., Efros, A.A., Darrell, T.: Curiosity-driven exploration by self-supervised prediction. In: Proceedings of the 34th International Conference on Machine Learning (ICML), vol. 70 (2017)
- [51] Ng, A.Y., Harada, D., Russell, S.: Policy invariance under reward transformations: Theory and application to reward shaping. In: Proceedings of the 16th International Conference on Machine Learning (ICML) (1999)

## Methods

### Canonical ensemble via ERGM

ERGM defines a graph distribution  $P(G)$  on a graph space  $\mathcal{G}$  by maximizing the Shannon entropy subject to soft constraints  $\langle C_i(G) \rangle = c_i$ , yielding

$$P(G) = \frac{1}{Z} \exp \left( \sum_i \lambda_i C_i(G) \right), \quad (5)$$

where  $\lambda_i$  are conjugate parameters for the corresponding constraints  $C_i$  and  $Z$  is the partition function.

To sample from Eq. (5) under the assortativity constraint, we employ the Metropolis–Hastings (MH) algorithm. In each step, a degree-preserving rewiring is proposed by selecting two edges,  $(u, v)$  and  $(x, y)$  uniformly at random and rewiring them to either  $\{(u, x), (v, y)\}$  or  $\{(u, y), (v, x)\}$ , denoted by modes  $b \in \{0, 1\}$ . As described in the main text, this proposal is accepted with probability  $\min[1, \exp(\lambda \Delta K)]$ . By evaluating the unnormalized increment  $\Delta K$  rather than the exact  $\Delta \rho$ , the MH algorithm targets the assortativity constraint while avoiding the computation of system-size dependent normalization factors.

The number of required rewirings  $T$  in ERGM is defined as the duration of the transient regime. We estimate it by identifying the time when the smoothed ensemble average of  $\rho$  settles within the

fluctuation band of the steady state. In this sense,  $T$  is the time when the initial transient bias has decayed below the level of stationary fluctuations.

For every ERGM result plotted as a function of  $\rho$  in the main text, we first tune the conjugate parameter  $\lambda$  such that  $\langle \rho \rangle$  matches the target assortativity. Reported statistics are derived from equilibrium configurations at the corresponding  $\lambda$ . Accordingly, for ERGM,  $\rho$  should be understood as the expected value, unlike the realized value in DMGG, which is constrained to lie within the target tolerance window.

To estimate the feasible assortativity interval associated with a given degree sequence, we use an empirical search. Starting from a given graph of  $E$  edges, we repeatedly propose random rewirings and accept only those that increase  $\rho$ ; after  $50E$  rewiring attempts, the resulting assortativity is taken as an empirical estimate of the maximum feasible value. Repeating the same procedure while accepting only moves that decrease  $\rho$  gives the corresponding empirical minimum.

### DMGG architecture and training

DMGG casts graph generation as a sequential rewiring process guided by a learned policy. At step  $t$ , the graph  $G_t$  is represented by its edge list and normalized node degrees  $k_i/k_{\max}$ . This representation proves sufficient for the task, avoiding the computational overhead associated with complex graph encodings. Crucially, the policy network is conditioned solely on the sign of the gap,  $\text{sgn}[\rho^* - \rho(G_t)]$ , a design choice that enables the model to extrapolate to target assortativities beyond the training region. In contrast, the value network receives the full gap to estimate the effective distance to the target, quantifying the remaining rewirings to reach the target manifold.

A rewiring action  $a_t = (e_1, e_2, b)$  involves selecting two distinct edges  $e_1, e_2$  and a rewiring mode  $b$ . Since the number of valid rewirings scales as  $O(E^2)$ , the resulting combinatorial explosion renders direct scoring of all possible rewirings computationally intractable. We therefore adopt a factorized policy architecture [46]:

$$\pi(a_t|G_t) = \pi_1(e_1|G_t) \cdot \pi_2(e_2|e_1, G_t) \cdot \pi_b(b|e_1, e_2, G_t). \quad (6)$$

Each conditional distribution is parametrized by a separate neural network, reducing the output

dimension from quadratic to linear in the number of edges.

To ensure physical validity, we implement action masking [47], setting the probabilities of invalid rewirings to zero before sampling the action. Furthermore, rewirings that leave  $K(G)$  unchanged are also masked, as they do not contribute to controlling  $\rho$ . If this restriction empties the action set, the mask is relaxed to enforce only validity constraints.

A graph neural network built from GIN layers [48] with FiLM conditioning [49] extracts hidden features from  $G_t$  and  $\rho^*$ , which are then fed to the three policy heads and value network. Target assortativities are sampled from the feasible interval of the given degree sequence with a small margin from the extremal values. We implement a physically confined tolerance threshold

$$\varepsilon_{\text{phys}} \equiv \max\left(\varepsilon, \frac{2}{E \cdot \text{Var}(k)}\right), \quad (7)$$

where the second term accounts for the minimum change of  $\rho$  by a single rewiring in finite systems. This correction dominates only in small graphs where single rewiring steps induce changes comparable to the given  $\varepsilon$ .

The learning process is driven by a reward signal that the policy seeks to maximize. However, relying solely on a binary indicator for hard constraint satisfaction introduces the fundamental challenge of reward sparsity [50]. To address this, we utilize reward shaping based on a potential function defined in the configuration space [51]:

$$\phi_\zeta(\rho, \rho^*) \equiv \frac{|\rho^*| + \zeta}{|\rho^* - \rho| + \zeta}, \quad (8)$$

where  $\zeta > 0$  controls the gradient sharpness near the target  $\rho^*$ . This potential is normalized such that  $\phi_\zeta(0, \rho^*) \approx 1$  for initial graphs. For notational simplicity, we denote  $\phi_\zeta(\rho, \rho^*)$  as  $\phi(\rho)$ . The reward  $r_t$  at step  $t$  is then defined as

$$r_t = [\phi(\rho_t) - \phi(\rho_{t-1})] - p + s \cdot \mathbb{1}_{[\rho^* - \varepsilon, \rho^* + \varepsilon]}(\rho_t), \quad (9)$$

where  $p > 0$  is a step penalty,  $s \gg 1$  is a success bonus, and  $\mathbb{1}_A(\cdot)$  represents the indicator function. The potential difference term provides dense feedback to guide the policy toward the target, while the step penalty encourages rapid

convergence. Ultimately, the policy is optimized to maximize the cumulative reward  $\sum_{t=0}^T \gamma^t r_t$ , where the discount factor  $\gamma \in (0, 1)$  balances immediate and future rewards. Training was performed using PPO with  $\gamma = 0.997$ ,  $\zeta = 0.005$ ,  $p = 0.001$ , and  $s = 100$ .

## Acknowledgements

This work was supported by the National Research Foundation of Korea (NRF) grant funded by the Korea Government (MSIT) No. RS-2025-00556024 (H. C.) and No. 2022R1A2C1006871 (J. J.), and by a KIAS Individual Grant No. CG079902 (D.-S. L.) at Korea Institute for Advanced Study. This work is supported by the Center for Advanced Computation at Korea Institute for Advanced Study.

## Declarations

**Author contribution.** H. Y. Choi conceptualized the study, developed the methodology, conducted numerical experiments, analyzed the results, and wrote the original manuscript. J. Jo and D.-S. Lee supervised the project, provided scientific guidance and feedback throughout the study, and critically reviewed and revised the manuscript. All authors read and approved the final manuscript.

**Competing interests.** The authors declare no competing interests.

**Data availability.** The data supporting the findings of this study are reproducible using the code described in the Code Availability section. No additional datasets are required.

**Code availability.** The code used in this study is provided as Supplementary Information accompanying this manuscript and will be publicly available at <https://github.com/hoyunchoi/DMGG> upon acceptance.